Cooling of a structured high temperature surface with a dispersed flow

Valentin Shteling*, Alexander* Komov*, Petr* Shcherbakov*, Alexander* Zakharenkov *and* Andrey *Sliva*

National Research University "MPEI", 111250, Russia, Moscow, st. Krasnokazarmennaya, 14

Abstract. The authors have conducted an investigation into the cooling of five distinct types of structured surfaces by means of a dispersed flow of distilled water. The modification of the heat transfer surface of the copper working section was conducted using a variety of methods, including mechanical processing and electron beam treatment at different parameters. Macrophotographs of the structured surface were obtained and their profiles were subsequently measured using a profilometer. Two series of experiments were conducted for each surface, with different coolant parameters. The excess pressure of the coolant at the nozzle inlet was in the range of 1.5 to 3.5 × 10^5 Pa, the mass flow rate of the coolant (distilled water) was in the range of 4.0 to 6.1 × 10^{-3} kg/s, and the irrigation density varied within the range of 4.2 to 6.2 kg/(m²·s). The relationships between heat flux and heat transfer coefficient were compared for both modified and unmodified surfaces. The calculated thermophysical quantities were also represented graphically.

1 Introduction

The rapid development of powerful electronic, power plants and engines has led to the fact that the characteristics of these systems have become limited by the heat removal capabilities. [1] No less urgent is the issue of cooling of modern power systems, including advanced fusion plants, where, according to estimates, it is also necessary to provide heat removal of megawatt loads. [2]

The thermal loads on current and future electronics and fusion reactor facilities are so great that conventional single-phase convection cooling has reached its limit. In this case, phase transition cooling, which utilizes the latent heat of vaporization, must be applied. [3]

Among various methods of phase transition cooling, spray cooling has the best combination of heat removal efficiency and homogeneity of temperature values. The method under consideration has found wide application in cooling of various elements of power electronics. [4,5]

Nevertheless, the heat transfer and heat dissipation efficiency of spray cooling need further improvement to meet the requirements of next generation ultra-high-power applications. The development of surface properties and structures enabled by modern manufacturing techniques can significantly influence the interaction between the dispersed flow and the cooled wall. However, the mechanisms of spray cooling with improved thermophysical surface properties are varied and ambiguous. In this work, the cooling of

Corresponding author: schteling@gmail.com

various structured surfaces by dispersed distilled water flow was investigated on an experimental stand modelling energy-loaded elements of fusion plants. A detailed description of the experimental bench and characteristics of the working section is given in [6]. The area of the heat exchange surface of the working section is 7 cm^2, which significantly exceeds this parameter in similar works.

2 Characteristics of structured surfaces

In order to examine the phenomenon of heat transfer in the context of dispersed flow, a total of six distinct structured surfaces were created, encompassing both unmodified and modified variants. These surfaces were produced through the utilisation of diverse techniques and processing tools. Macrophotographs were obtained for these surfaces, and a roughness profile was obtained for those structures for which this was feasible. A MarSurf PS10 profilometer was employed to obtain the roughness profile, which has a maximum measurement range of 350 μm and a profile resolution of up to 8 nm. Fig. 1 presents photographic images of the resulting structured surfaces. Furthermore, the study presents a comparison of heat transfer on structured surfaces with that on an unmodified surface, represented by a technical surface machined with a face cutter and exhibiting the following roughness parameters: The surface roughness was found to be 7.39 μm for R_z and 1.18 μm for R_a. The roughness profile of the unmodified surface is illustrated in fig. 2(a).

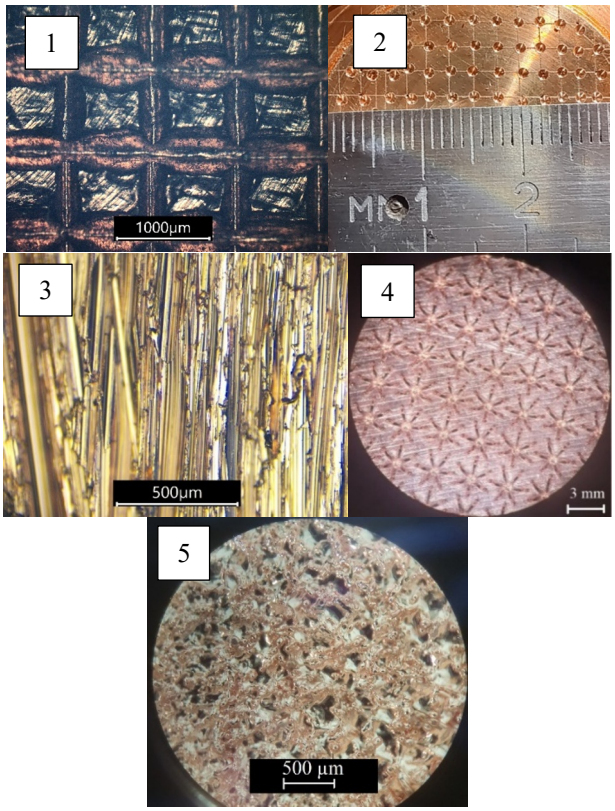

Fig. 1. Photographs of structured surfaces: 1 – knurling modification; 2 – modification with wells; 3 – modification with abrasive material; 4 – macrostructure obtained by electron beam processing; 5 – microstructure obtained by electron beam processing

The following section presents the measured roughness profiles of the structured surfaces, which have been modified for a better understanding of their modification (fig. 2).

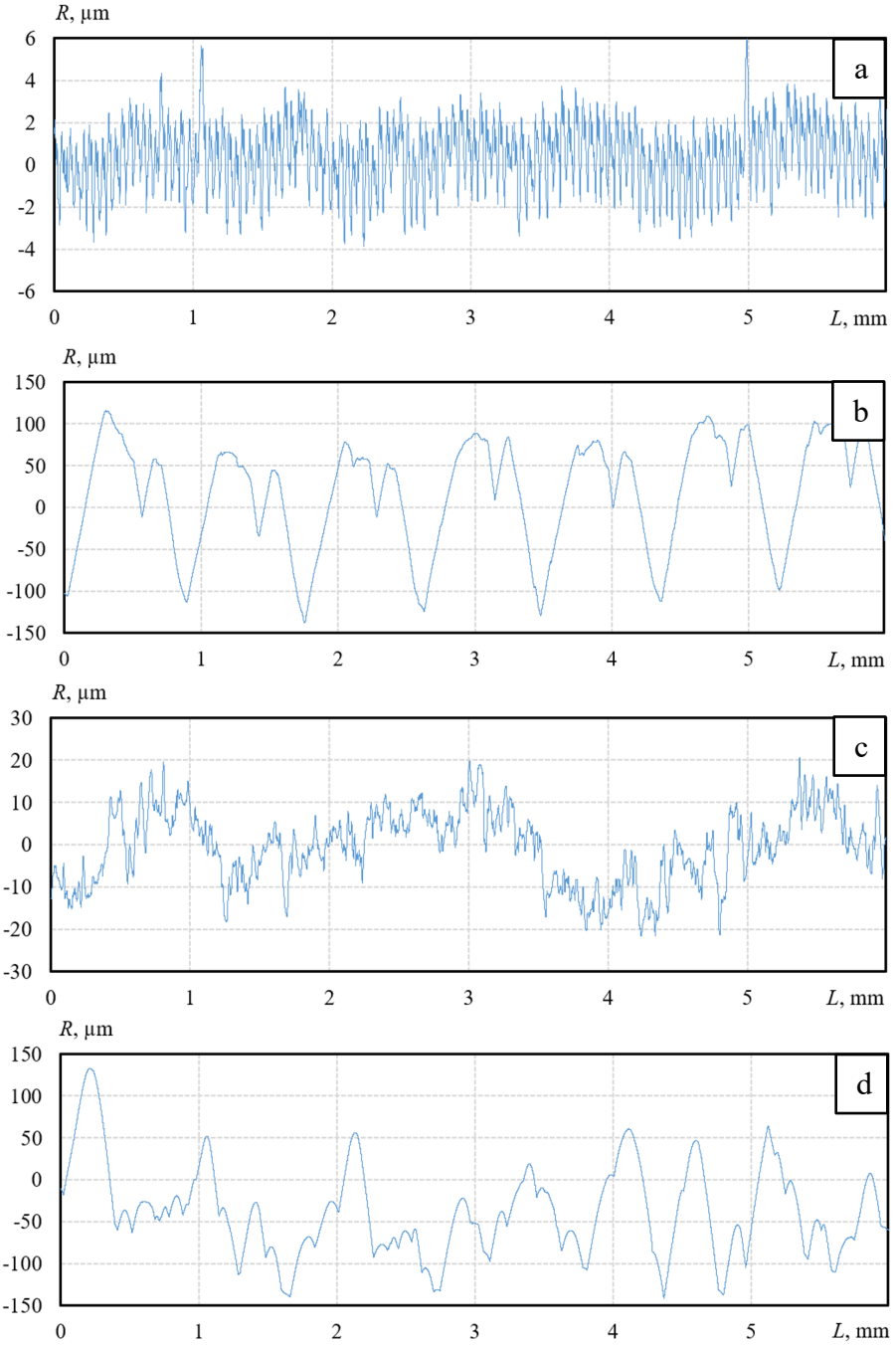

Fig. 2. Surface roughness profiles: a – unmodified surface; b – knurling modification; c – modification with abrasive material; d – microstructure obtained by electron beam processing

2.1 Surface modified by knurling of structures

The first surface (see fig. 1.1) was modified using a knurling roller with a single straight notch and a pitch of 0.8 mm. The structures were rolled in a sequential manner, both in the transverse and longitudinal directions.
The roughness parameters in the transverse direction are as follows: R_z = 144,19 μm; R_a = 30,93 μm; The roughness parameters in the longitudinal direction were as follows: R_z = 142,68 μm; R_a = 36,62 μm. The roughness profile of the aforementioned surface is illustrated in fig. 2(b).

2.2 Surface modified with wells

The second surface was made by drilling 1 mm diameter wells (fig. 1.2). The distance between the wells is 1.5 mm. As the scale of the structures exceeds the measurement capabilities of the profilometer, a schematic representation of their geometry and characteristic dimensions is provided in Fig. 3.

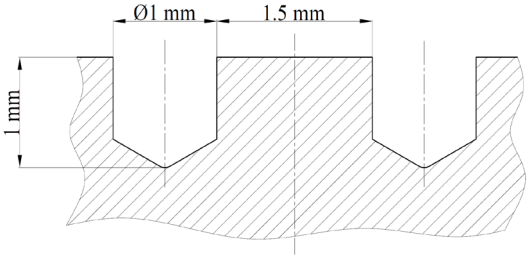

Fig. 3. Profile of the surface modified with wells

2.3 Surface modified with abrasive material

The third surface (see Figure 1.3) was modified with an aluminium-oxide abrasive on a flexible base with a grain size of 400-500 μm. The roughness parameters in the transverse direction are as follows: R_z = 30.45 μm; R_a = 4.38 μm; The roughness parameters in the longitudinal direction are as follows: R_z = 22.09 μm; R_a = 3.13 μm. The roughness profile of this surface is shown in fig. 2(c).

2.4 Macrostructured surface obtained by electron beam treatment

The fourth surface was modified at the technological complex for materials processing using an electron beam (ALTK-344-12) with an accelerating voltage of 60 kV. The trajectory of the beam is illustrated in figure 4. The numerical values indicate the sequence of movement of the electron beam along the trajectory. The processing modes employed were as follows: an electron beam current of 10 mA, a sweep frequency of 100 Hz, a sweep amplitude of 3 mm (with a beam length of 1.5 mm), and a processing time of 1 s for each structural element.

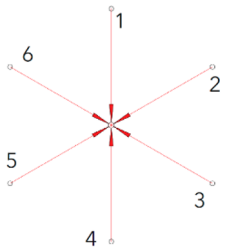

Fig. 4. Schematic of the electron beam sweep

In such a sweeping motion, the liquid metal shifts to the periphery of the beams, thereby forming a depression in the middle. Consequently, a structure in the shape of a six-beam star, comprising six peaks at the edges of the beams and a depression in the centre, emerges on the treated surface (see fig. 1.4). The maximum depth of inhomogeneities is 500 μm.

2.5 Microstructured surface obtained by electron beam treatment

The fifth surface was also subjected to processing on the electron beam machine ALTK-344-12. In order to process the surface, a sweep of the "pulse" type was employed. This type of sweep entails the movement of the electron beam with a defined step size between points, thereby increasing the cooling rate. In order to minimise the thermal influence of the neighbouring point, the surface filling was carried out with the use of skips and subsequent return to the neighbouring point. In order to achieve this method, the electron gun was moved continuously at a constant speed, while the electron beam was deflected in a pulsed mode. The surface treatment was conducted at a speed of 1500 mm/min, with a sweep frequency of 24 Hz and a beam current of 65 mA. The duration of the action period for a single pulse is 0.4 milliseconds. The surface exhibits an aperiodic structure formed by droplets of molten and crystallised metal, with a size range of 50 to 150 μm (see Figure 1.5). The surface's roughness parameters in the transverse direction are as follows: R_z = 132.93 μm; R_a = 25.80 μm. The surface's roughness parameters in the transverse direction are as follows: R_z = 144.82 μm; R_a = 32.26 μm. The roughness profile of the surface is illustrated in fig. 2(d).

2.6 Summary table of scaling characteristics of surfaces

The table of surface characteristics is provided below for reference. The numbering of surfaces is employed in subsequent graphical representations of the thermophysical characteristics of heat exchange between these surfaces and a dispersed coolant flow. The average size of surface structures was estimated for surfaces displaying structures of a scale exceeding the limits of the profilometer, employing the method of applying these structures. The mean size of the remaining structures is taken to be equal to the mean roughness value, R_z. Given that the average Sauter diameter d_{32} of the droplets forming the spray, which originate from the nozzle used, is in the range of 85 to 95 μm and decreases with increasing pressure, it can be assumed that the surface structures are in contact with the dispersed coolant over their entire surface area.

Table 1. Summary table of scaling characteristics of surfaces.

№	Surface type	Average value R_a, μm	Average value R_z, μm	Average size of surface structures, μm
1	Unmodified surface	1.18	7.39	7.39
2	Knurling modification	33.78	143.44	143.44
3	Modification with wells	-	-	1000
4	Modification with abrasive material	3.755	26.27	26.27
5	Macrostructure obtained by electron beam processing	-	-	500
6	Microstructure obtained by electron beam	29.03	138.88	138.88

3 Experimental results of the study of heat exchange of structure surfaces with dispersed coolant flow

3.1 Methodology for calculation of thermophysical characteristics

The methodology employed in the experimental study is elucidated in great detail by the authors in reference [6]. The methodology employed for the calculation of the results of the experiments is outlined below.

In order to evaluate the efficiency of the heat transfer process, the heat flux and the heat transfer coefficient were calculated for each experimental mode.
The heat flux is calculated as follows:

$$q = \lambda \frac{\overline{T}_2 - \overline{T}_1}{x_2 - x_1} \qquad (1)$$

where $\overline{T}_1, \overline{T}_2 -$ is the average temperature in cross-sections x_1 and x_2 of the working section, λ is the thermal conductivity of the material of the working section (copper M1).
The heat transfer coefficient is estimated as follows:

$$\alpha = \frac{q}{\Delta T_w} = \frac{q}{T_w - T_s} \qquad (2)$$

where T_w is the wall temperature, and T_s is the saturation temperature of water at atmospheric pressure.

3.2 Experimental results

Fig. 5 illustrates the experimental dependences of heat flux on wall superheat for all surfaces under identical regime parameters of the coolant. As illustrated in the dependence, the most pronounced augmentation in heat flux for the modified surfaces is discernible within the range of wall superheat between 20 and 30 °C. The critical heat flux for all surfaces, including

those that have not been modified, shows only minor fluctuations and differs by no more than 5%.

The greatest increase in the heat transfer coefficient (fig. 6) is also observed in the region of wall superheat from 20 to 30 °C. Conversely, when wall superheat reaches 50 °C, the heat transfer coefficient for all surfaces decreases to a value that is almost identical.

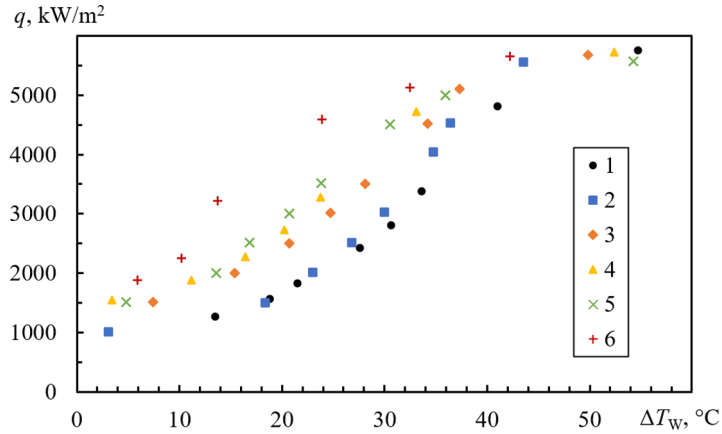

Fig. 5. Heat flux dependence on wall superheat. Coolant parameters for each mode $p = 1.5 \cdot 10^5$ Pa, $G = 4.0 \cdot 10^{-3}$ kg/s, $j = 4.2$ kg/(m²·s). Designations of various modified surfaces in accordance with table 1

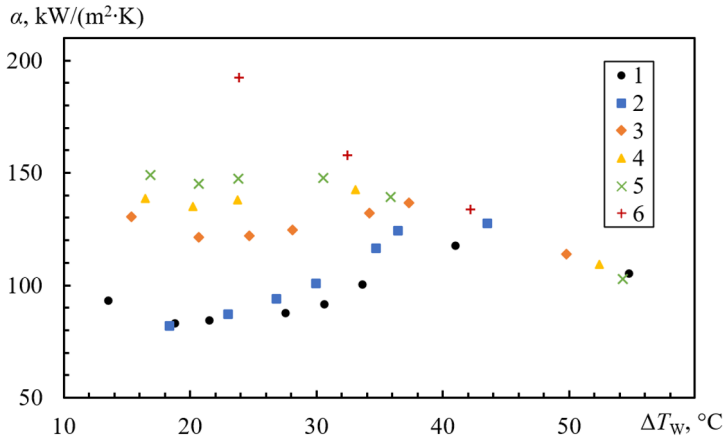

Fig. 6. Heat transfer coefficient dependence on wall superheat. Coolant parameters for each mode p = $1.5 \cdot 10^5$ Pa, G = $4.0 \cdot 10^{-3}$ kg/s, j = 4.2 kg/(m²·s). Designations of various modified surfaces in accordance with table 1

Fig. 7-8 illustrate the experimental dependences of heat flux and coefficient on wall superheat for all investigated surfaces at an elevated flow rate and coolant pressure. The greatest enhancement in heat transfer efficiency is also observed within the range of wall superheat from 20 to 30 °C. Nevertheless, an increase in coolant flow rate gives rise to a comparatively smaller relative increase in heat flux and heat transfer coefficient for the modified surfaces in comparison to the unmodified surface. The following section presents a summary of the impact of diverse surface modifications on heat transfer in the context of dispersed coolant flow.

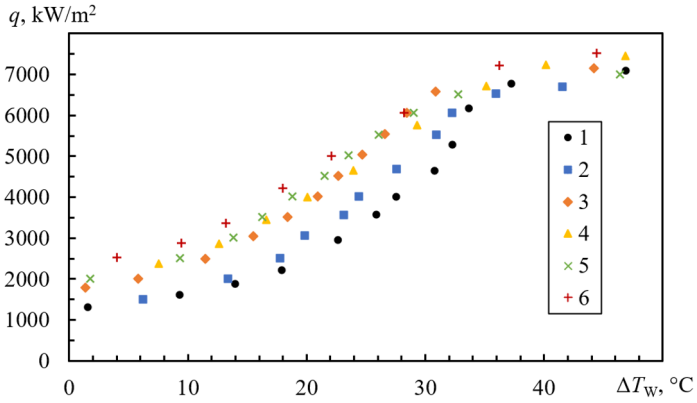

Fig. 7. Heat flux dependence on wall superheat. Coolant parameters for each mode p =3.5·10^5 Pa, G = 6.1·10^{-3} kg/s, j = 6.2 kg/(m^2·s). Designations of various modified surfaces in accordance with table 1

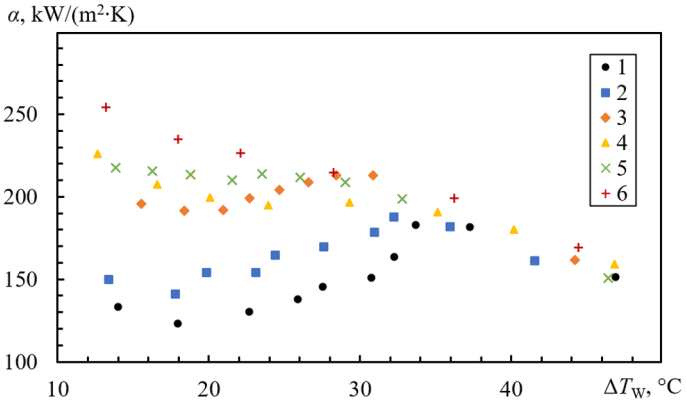

Fig. 8. Heat transfer coefficient dependence on wall superheat. Coolant parameters for each mode p =3.5·10^5 Pa, G = 6.1·10^{-3} kg/s, j = 6.2 kg/(m^2 ·s). Designations of various modified surfaces in accordance with table 1

3.3 An analysis of the impact of surface modifications on the efficiency of heat exchange with dispersed coolant flow

Table 2 illustrates the comparative values of the maximum increase in thermophysical characteristics for all investigated surfaces in relation to the unmodified surface, at two distinct coolant regime parameters.

Table 2. Summary table of the impact of various surface modification techniques on the efficiency of heat transfer at a constant wall superheat

	Coolant parameters →	*p*, Pa	*G*, kg/s	*j*, kg/(m²·s)	*p*, Pa	*G*, kg/s	*j*, kg/(m²·s)
		$1.5 \cdot 10^5$	$4.0 \cdot 10^{-3}$	4.2	$3.5 \cdot 10^5$	$6.1 \cdot 10^{-3}$	6.2
№	Surface type ↓	Increase in *q*, %		Increase in *α*, %	Increase in *q*, %		Increase in *α*, %
1	Unmodified surface	–		–	–		–
2	Knurling modification	20		17	18		26
3	Modification with wells	48		45	49		53
4	Modification with abrasive material	64		60	50		54
5	Macrostructure obtained by electron beam treatment	75		73	65		65
6	Microstructure obtained by electron beam treatment	125		120	80		94

The analysis of the obtained data allows us to conclude that an increase in the flow rate and pressure of the coolant results in a reduction of the increase in the removed heat flux and heat transfer coefficient on some surfaces. This effect is particularly pronounced in the microstructure obtained through electron beam treatment. Nevertheless, this structure exhibits the highest heat transfer efficiency of all the modifications presented. This is due to the fact that its most developed surface area is the largest reduced heat transfer area. This surface characteristic results in a notable reduction in surface temperature, accompanied by a comparable heat flux, which in turn gives rise to a considerable enhancement in the heat transfer coefficient, in comparison to the unmodified surface. Additionally, the developed surface structure, comprising numerous microstructures, is likely to enhance the boiling process of the liquid film formed by dispersed flow of the heat exchange surface. However, this phenomenon requires further investigation.

The reduction in the impact of structures on heat transfer efficiency with rising coolant flow rates is likely attributable to the rise in the proportion of convective heat transfer and the decline in the proportion of phase transition heat transfer. Therefore, the enhancement of heat transfer by surface structures due to the intensification of the boiling process becomes less effective with increasing coolant flow rate. This is corroborated by the findings pertaining to surfaces that have undergone modification through the introduction of wells and knurling (2, 3). As the coolant flow rate increases, the efficiency of these structures is maintained due to their large size, which increases the reduced area and has a positive effect on convective heat transfer. However, their efficiency remains lower than that of surfaces with a more developed structure (4, 5, 6).

The modification with abrasive material (4), although seemingly straightforward, also results in a notable enhancement in the heat flux, comparable to the macrostructure achieved through electron beam treatment (5). Despite the considerable disparity in the scale of these structures, they exhibit comparable efficiency, which can be attributed to the intricate mechanisms governing the exchange of heat in a dispersed flow with a heated surface.

4 Conclusions

- The application of microstructures on the surface by electron beam resulted in an increase in the heat flux at low surface superheating relative to the saturation temperature by 125% relative to the unmodified surface. The heat transfer coefficient exhibited a 120% increase.
- It can be expected that the increase in heat transfer efficiency for surfaces containing microscale structures will be significantly reduced as the flow rate of dispersed coolant increases.
- The critical heat flux at cooling by dispersed coolant flow of the structured surface remains largely unchanged and is not dependent on the specific type of modification.
- The selection of the optimal characteristics of the structured surface for cooling by dispersed flow is largely dependent on the parameters of the dispersed flow and the conditions of application of this type of cooling.
- The substantial reduction in temperature observed in structured surfaces relative to unmodified surfaces at identical heat flux values is a valuable outcome in modern power systems. It enables the mitigation of thermal loads on the most energy-intensive components, enhancing the overall efficiency of the system.

Funding

This work was financially supported by the Russian Science Foundation (agreement no. 23-19-00476).

References

1. A. Bar-Cohen, J.J. Maurer and J.G. Felbinger, Darpa's intra/interchip enhanced cooling (icecool) program. International Conference on Compound Semiconductor Manufacturing Technology, CS MANTECH. 171-174 (2013)
2. A. Vertkov, M. Zharkov, I.E Lyublinski, A. Berlov, I. Tazhibayeva, Y. Ponkratov and Y. Gordienko, New version of lithum divertor of KTM tokamak. 42. 5-13. (2019)
3. G. Liang and I. Mudawar, Review of spray cooling – Part 1: Single-phase and nucleate boiling regimes, and critical heat flux. Int. J. Heat Mass Transfer. **115**, 1174-1205 (2017)
4. S. S. Hsieh and S. Y. Luo, Droplet Impact Dynamics and Transient. Heat Transfer of a Micro Spray System for Power Electronics Devices. Int. J. Heat Mass Transfer, **92**, 190–205 (2016)
5. K. Bloschock and A. Bar-Cohen Advanced thermal management technologies for defense electronics. Proceedings of SPIE - The International Society for Optical Engineering. **8405**. (2012)
6. A.T. Komov, A.V. Dedov, P.P. Shcherbakov, A.V. Zakharenkov, V.S. Shteling and A. D. Sokolova, Heat transfer of a modified surface with a dispersed coolant flow. E3S Web of Conferences. **459**. (2023)